***

NEUTRON AND HEAT GENERATION INDUCED BY ELECTRIC DISCHARGE

Tadahiko Mizuno, Tadashi Akimoto[1], Tadayoshi Ohmori [2]

ABSTRACT

Production of low energy neutrons was confirmed during electrolytic discharge at high voltage in a heavy water solution. We employed a He^3 neutron detector and a NE-213 scintillator to measure neutron emission and energy distribution. We counted several thousand thermal neutrons per second. High heat output of the order of 20% above input power was observed from input power of tens of watts. The neutron counts detected by the He^3 detector increased with discharge time after an induction period, and showed radical fluctuations. Absorption of neutrons by cadmium showed them to be thermal. Copper and iron showed no count changes. The ratio of fast neutrons was shown, by the NE-213, to be 0.01%. These figures were estimated from a count observed to be 30% above background (0.048/s and 0.036/s respectively). We found only 0.14 counts per second of neutron emissions from the electrode above the 0.7 MeV level. The values are estimated from their counting differences and the efficiencies of the detecting equipment. The neutron emission rate corresponded linearly with the input current, except at the low input Coulomb range due to induction time. From this linear relation, it was observed that the typical dependence of neutron emission/current during 1 hour was 3500 / s / A/cm^2 for a platinum electrode. We conclude that a nuclear reaction was induced by the electric discharge on the metal surface in the solution. The reaction probably took place in the thin layer between the electrolyte and electrode.

INTRODUCTION

Many researchers have reported nuclear reactions in a solid electrode at ambient temperatures since 1989 [1-3]. Replication of the process requires highly sophisticated control techniques. This complication, coupled with inexplicit understanding of cold fusion reactions generally has resulted in the reality of the phenomenon failing to achieve wide acceptance.

Early researchers seeking to replicate the results Fleischmann and Ports achieved in 1989 may have been too rigid in their experimental procedures, using exclusively the materials specified by that particular experiment, or only using other metals with high hydrogen absorption properties.

In our experiments we used electrodes constructed from Ti, Ni and the alloy LaNi, preferring to use an alkaline Li solution as the electrolyte for the purpose of maximizing the potential of the electrolytic reaction. Generally, we measured the current density in the electrode area to be several hundred amperes with an input of several tens of volts.

Subsequent researchers, assuming their observed reactions to be nuclear fusion, concentrated their efforts solely on the detection and measurement of the daughter products of fusion such as thermal heat, neutron, tritium charged particles, and radio emissions. The only reaction they considered was fusion. We did not restrict ourselves to seeking only fusion byproducts, we carefully measured and noted all observed effects, frequently even adapting our measurement technique to ensure accuracy and precision.

[1] Department of Quantum Energy, Faculty of Engr., Hokkaido Univ., Kita-ku Kita 13, Nishi 8, Sapporo 060 Japan.

[2] Catalysis Research Center, Hokkaido University, Kita-ku 10, Nishi 9, Sapporo, 060 Japan.

If an electrochemical process induces nuclear reactions, there ought to be clear evidence of radiation or isotopic changes and it would be possible to define such effects in terms of accepted theory. We have demonstrated that isotopic changes occurred within the reaction products deposited on the electrode surface. Such transfigurations cannot be regarded as the result of impurities within the system, the total amount of which had been carefully measured prior to and following experimentation. We attempted to explain the production of these anomalous products within the framework of the accepted theory. In this way we show the relationship between production of heat, neutrons, and other products following the electrolytic processes.

EXPERIMENTAL

The Pt wire and mesh electrode was of the highest quality (99.99% pure, supplied by Tanaka Precious Metals Ltd.). The trace impurities, above the limits of detection, were Rh at 18 ppm; Si, Cr, Pd each at 2 ppm and Au, Ag, B, Ca, Cu, Fe all at less than 1 ppm. The heavy water used (99.75% pure, supplied by Showa Denko Ltd.) contained 0.077 micro Curie cm^{-3} tritium, was purified in a quartz glass distiller before the addition of a reagent. High purity lithium hydroxide (produced by Merck Ltd.) contained Cl and SO_4, both at 10 ppm and SiO_4 and Ba both at 5 ppm. Other trace impurities were all below the 0.1 ppm level.

The electrolytic cell and measurement systems are shown schematically in Fig. 1. The cell measured 6 cm in diameter and 15 cm in height. The cathode comprised a rectangular Pt plate (0.5 cm x 1.0 cm) and incorporated a 15 cm length of Pt wire. The anode, also rectangular Pt had an integral lattice constructed using a 15 cm length of 0.I cm diameter Pt wire. Teflon tubing encased the adjacent surfaces to prevent any explosive H-O recombination reaction occurring within the cell. The cell had a Teflon cap with openings to allow the insertion of cables and thermocouples.

A Teflon-coated stainless steel heater calibrated the temperature to compute power-input ratio. Heater output was typically 300 watts and temperatures ranged from 45° to 95°C. The homogeneity of the electrolyte was facilitated by use of a rotating Teflon-encased iron stirrer driven magnetically from beneath the cell. The temperature: power-input results obtained from this arrangement were correlated with those of previous experiments. The thermal effects of vapor release from the top of the cell had not been allowed for during calibration, therefore, at higher input levels, with the attendant possibility of electrical discharge, heat output levels needed to be underestimated. Three K-type thermocouples sheathed in Teflon film recorded the temperature levels at distinct points within the cell. Temperature levels were collected by a computer-linked data logger (R7326B, made by Advantest Ltd.). Environmental conditions were regulated by encasing the cell within an incubator (Yamato IL-61) which maintained a constant temperature of 23°C.

We used a Takasago Products Ltd., EX-I500L unit to supply DC power ranging upward to maximum levels of 25A and 240v. The data logger converted input levels into a digital format acceptable to the computer software and the input voltage was directly measured between the two electrodes of the cell. Heat created by the power supply during lengthy neutron detection runs, was dissipated by means of an electric fan. We carried out a trial run of 30 minute duration with input levels of 60v and 3A in order to remove impurities from the electrolyte.

The measurement of neutron levels was carried out by a He^3 survey meter (TPS-451S, Aloka Ltd.) at energy dependencies of 1.5 s^{-1} / micro Sv/h^{-1} from 0.025 eV of thermal and 10 keV. A substantial increase was noted in the fast neutron range of 15 MeV. The detector is spherical in shape, with a diameter of 30 cm, and has a block of controls to the front of the device. The signal is output through a counter scalar. Measurement of the neutron energy spectrum was handled by a NE-213 scintillator, previously described [4]. The detectors were calibrated to the standard level of 20 micro Curie using a Cf-252 source. The total efficiencies including intrinsic and geometrical factors for He^3 and NE-213 system were 0.001 and 0.07 respectively for the calibrated energy range.

We employed the rise-time discrimination technique to eliminate noise induced by gamma radiation, and by the electrical and thermionic side effects of the photo multiplier. A transducer was used to reduce emanations from the two power supplies in order to prevent noise pollution from that source interfering with the neutron measurement apparatus. A liquid scintillator of NE-213 (proton recoil detector, 12.7 cm diameter x 12.7 cm length) analyzed the energy spectrum of the neutrons. Thermal neutron absorption was facilitated by the use of a metal sheet plated with an alloy of cadmium, copper and iron, 30 cm x 30 cm x I mm thick This had the added advantage of also acting as an electrical noise shield.

To verify levels of gamma and x-ray emission, a GM survey meter (TGS-11, Aloka Ltd.) was used both during and following electrolytic discharging. Existence of neutron emission was confirmed by siting a rectangular gold plate, 2 cm x 2.5 cm x 0.5 mm thick, close to the cell. After 6 hours exposure, the plate was examined using gamma spectroscopy.

RESULTS

1. Electrolytic light emission

Fig. 2 shows a typical correlation between applied voltage and current in the 0.1 mol lithium hydroxide solution. Cathodic current increased linearly to 10 A/cm^2 with an input power of 80 volts. At around the 100 volt input level, a considerable quantity of hydrogen gas and vapor was expelled from the cell, the electrode emitted a resounding rumble and the current became very unstable. At just over 120 volts the current decreased sharply and, simultaneously, the electrode became bathed in an intense pink light. Typical light emission levels are shown in Fig. 3; spectroscopic examination of the sample plate confirms these radiance levels. This, previously observed, electrolytic light emission was reported by Jasnorodski [5], Polakowski [6] and precise details of the mechanism of the phenomenon were reported by Owaku and Kuroyanagi [7] in the 1950's.

2. Neutron emission

Fig. 4 shows characteristic neutron measurement results. Neutron counts were taken at 10-second intervals from the data collected by the He^3 detector. Count levels showed a gradual increase with time at the onset of electrolytic discharging and then changed radically. An iron and copper plate, used to shield the detector from electric noise, did not alter the count levels achieved before its installation. However, the substitution of a 0.3 mm thick cadmium sheet caused a steep decline in the order of 1/l0th of previously recorded levels. It can be said, therefore, that electrolytic charging induced the slow neutron emission. At the same time, the NE-213 detected values of 0.048 count/s, 30% in excess of the 0.036 count/s background level. Adjusted for sensor efficiency, thus 0.14 counts per second of high-energy neutron emissions were observed from the electrode above the 0.7 MeV level. This value is calculated allowing for counting differences and detector efficiency. The ratio of fast to total neutrons, measured by the He^3 and NE-213 detectors, is of the magnitude 10^{-4}.

The neutron emission rate corresponds linearly with the level of input current, as shown in Fig. 5, with the exception of the low input Coulomb range. This means that neutron emission began occurring after an unquantified induction period and then began to increase. From these data, we calculate the average number of emissions/hour to be 3500 count/s where electrical input to the electrode is 1.0 A/cm^2. The criterion used for neutron emission calculation was the same as that for the electron (5.6×10^{-16} cm^2), assuming electron discharge at the electrode surface was the impetus for the reaction. On this basis, we can calculate a reaction cross-section estimated from current density in the order 5.6×10^8. It was noted, however, that counts of gamma and x-ray emissions increased by 50% during discharging.

3. Neutron activation measurement

Fig. 6 shows the spectra of the gold plate before and after electrolytic discharge; the data, in both cases, being accumulated at 86,400 samplings per second. The clearly visible peak at 0.412 MeV derives from Au-198 gamma emission.

4. Excess heat evolution

Fig. 7 shows the results described in 4 above, together with the excess heat production measurements. In this instance, at a sampling rate of 10 per second, a constant 140 V input was maintained while the current was decreased from 8A to 0.4A within a period of 2000 seconds. Power input began at 1120 W and was reduced down to 56 W, during which time the temperature of the electrolyte rose steeply from 38°C to 90°C after a period of 1100 seconds. A temperature ceiling of 95°C was necessary as above this temperature there was a substantial release of vapor and gas from the cell, rendering excess heat estimation difficult.

Production of excess heat occurred 50 seconds after discharge and showed variations in level throughout the measurement period. We estimate the maximum value of excess heat observed to be 180 W after 100 seconds of discharge at an input level of 400 watts. Input and output energy was 145,903 and 154,080 joule respectively which gives us an excess heat measurement of 8,177 joule. Although this value only represents 5.6% of total input energy, it is significantly underestimated as the original calibration allowed no margin to correct for energy lost through gas and vapor release. Following this heat measurement experiment, the quantity of electrolyte was depleted by 10 grams. Using this data it is possible to approximate the rate of energy lost through vapor release as 30,815 joule, giving the measurement of excess energy as 20% of input power.

DISCUSSION

The relationship between the production of excess heat and neutron levels has been approximated from the experimental results. With excess heat at 8,200 joule and total neutron production at 3×10^6 , we can estimate the heat evolution for the neutron as 1.7×10^{10} MeV. The resulting value is excessive in comparison with the level at which conventional thermal-energy-producing nuclear reactions occur. We should have obtained 10^{12} - 10^{13} neutrons/s if the reaction remained strictly concordant with wattage levels. Conversely, we detected heat generation of the order 10^{-3} - 10^{-4} watts when observed neutron levels were 10^3 - 10^4. From these results, we concluded that an unusual reaction took place during discharging in that very few nuclear products were created when excess heat generation was at its highest recorded level. In postulating a mechanism for this reaction, we considered a likely occurrence might be that the majority of neutrons interacted with the nuclei of the electrode metal, becoming absorbed and evolving into new nuclei, even in instances where neutron generation was substantial.

This effect could be considered to be occurring in tandem with the electrochemical reaction. The interaction between an energetic proton and electron can be preceded by electrochemical hydrogen evolution. Enyo [8-10] reports that the effective hydrogen pressure at the hydrogen-evolving electrode is dependent upon the recombination of hydrogen atoms following the electrolytic process. The total hydrogen overpotential E_t is represented by the addition of two other components, i.e., $E_t = E_1 + E_2$; where E_1 and E_2 represent the discharge and recombination processes respectively. Application of the Tafel relationship equation shows the reaction scale of E_l to be much more protracted than that of E_2. The Nernst Equation enables us to estimate effective hydrogen pressure at the electrode, suspended in an alkaline solution, to be up to 10^{16} atm [11,12] for normal electrolysis. However, if total cell input reached 1 V at the current density of 0.2 A/cm^2 on a noble metal surface [13], Tafel lines would indicate a maximum 5×10^4 atm actual pressure. In this instance, we can estimate the total overpotential up to a level of 150V. When the overpotential realized at the electrode was estimated to be at least 1 V, the statistical pressure is assessed to be 10^{30} atm. We therefore calculate that the proton/electron distance narrowed considerably under such high pressure.

It remains a difficult task to explain the reaction, using established quantum mechanical theory. However, the origin of the mechanism may be traced back to Rutherford [14] who conceived this physical process and the new kind of interaction VN(r) which Conte [15] derived in Bi-quaternion Quantum Mechanics (BQM). The BQM enables us to address the basic features of the nuclear structure and also to introduce new data observed from interactions created by the neutron emission process during electrical discharge. Conte explains that the theory can be fundamentally explained using a generalization of the Schrodinger equation. Here, we can show the theory briefly; a quantum action A = ! i h q log y is considered, where q is a bi-quaternion (the bi-quaternion are numbers that Conte has introduced in quantum mechanics, for a detailed derivation (see Eq. 1 and 2) and y is a wave function. This quantum action is a generalization of the usual quantum action B = ! i h log y by which the usual Hamiltonian H = ! dB/dt and the standard Schrödinger equation may be obtained.

When we consider the generalized action A instead of B, we obtain a generalized Schrödinger's equation that has the following form:

$$Ey = HTy \tag{1}$$

Where T is a proper bi-quaternion operator that assumes a particular form in consideration of the particular problem to be examined. As example, if we consider T given as it follows:

$$T = 1 ! * y \asymp y * \tag{2}$$

We obtain the non-linear Schrödinger equation formulated by N. Gisin to approach open quantum systems [16]. This is not, however, our case of interest. Consider, instead, a given system whose Hamiltonian is H and contains interactions deriving from a usual potential that we indicate by V(r). We have the usual Schrödinger equation.

$$E_u\, u = Hu \tag{3}$$

Let us return now to Eq. (1) and consider that the operator T is now given as follows

$$T = 1 ! * u \asymp u * \tag{4}$$

We may now insert Eq. (4) in Eq. (1) and we have

$$E\, y = H\,(1 ! * u \asymp u *)\, y \tag{5}$$

Or

$$Ey = (H ! E_u \langle u/y \rangle\ u/y)\, y \tag{6}$$

In other terms, the generalized Schrodinger equation (1) becomes

$$Ey = HN\, y \tag{7}$$

Where the new Hamiltonian

$$HN = H ! E_u \langle u/y \rangle\, u/y = H_0 + V(r) + VN(r) \tag{8}$$

is now given and it contains the new interaction

$$VN(r) = ! E_u \langle u/y \rangle\, u/y \tag{9}$$

Eq. (9) forms the basis of this discussion. VN(r) is a new, natural form of attractive interaction as derived by the BQM generalized Schrödinger Eq. (1). It is important to note that the equation is not written in the customary manner, as it does not represent the usual interaction deriving from a potential. The salient

feature in Eq. (9) is the expression <u/y>, which has a new and categorical meaning. This new interaction is due to mutual overlap of the involved wavepackets u and y.

This is truly a new and natural phenomenon. We are convinced that this relationship can explain all anomalies observed in nuclear reactions following electrical discharge. We would repeat that this interaction is unusual in that it is not derived from a potential, but is due solely to the mutual overlap of the involved wavepackets u and y.

Rutherford, in fact, conceived the neutron as a compressed hydrogen atom dominated by an interaction due to the total immersion of the wavepacket of the electron inside the dense medium of the proton. He considered the neutron to be a particle in a naturally bound state (anchored by the proton and the electron) at low temperature and at a short distance of under 1 fm. As we know, the existence of the neutron was confirmed by Chadwick in 1932, and that Rutherford's conception of the neutron was rejected because it did not comply fully with the laws of quantum mechanics, in that:
(a) there was a requirement for a positive binding energy (the neutron's mass being greater than that of the proton and electron);
(b) it was impossible to define the relatively large mean life of the neutron because of the diminutive mass of the electron and,
(c) the impossibility of giving the total spin ½ of the neutron from two component particles each of spin ½.

However, established quantum mechanical theory was essentially conceived to facilitate studies on atomic structure. On this level, the electron can be envisaged as being a point-like particle moving in vacuum. The physical conditions introduced by Rutherford and which we have now characterized in Eq. (9) are fundamentally different.

Eq. (9), in fact, characterizes the total immersion of the electron wavepacket inside the dense medium of the proton. A new explanation for this interaction is now required and we have thus applied a generalization of QM principles and, in particular, of the Schrödinger equation. As we discussed in Eqs.(2) and (3) this BQM theory fully resolves the problems posed in (a), (b) and (c) in the second preceding paragraph above which formed the basis of objection to Rutherford's original conception of the neutron

As we have shown in detail in Eqs. (2) and (3), if we consider that H of the Eq. (3) includes a usual potential interaction $V(r) = -e^2/r$ as it is the case of the proton and the electron, then we calculate consequently that $V_N(r)$ of the Eq. (9) assumes the following form:

$$V_N(r) = -k \exp(-ar) / (1 - \exp(-ar)) \qquad (10)$$

with $k > 0$ and constant.

Eq. (10) is well established in nuclear physics. It is referred to as the “Hulthen potential." In other words, in addition to the traditional interaction...and, in brief, the nuclear reaction in accordance with the following equation:

$$p^+ + e^- \text{ ---- } n + \text{neutrinos} \qquad (11)$$

Conte et al., have had direct experimental evidence confirming BQM and Eq. (11) from which reaction they have observed the experimental formation of the neutron. Other reported experimental results must also be considered. K. Kamada [17] performed experiments on electron impact p-p and d-d fusion in (hydrogen) molecules embedded in Al. Kamada used an ion implant technique to yield a high surface loading of hydrogen. Although Al does not absorb hydrogen in large quantities, it has a high hydrogen diffusion capability. It also has a rather high electro-negativity meaning that there are many available electrons. Kamada observed that when a suitably prepared hydrogen-implanted Al sample was bombarded with an intense electron beam at about 175 keV, high-energy charged particles were produced, representing reaction products at energy levels over 1 Mev. He also observed anomalous heat evolution in deuteron-implanted Al.

From Eq. (9), and in accordance with Eq. (11), we conclude that the following reactions: $e^{!} + p^{+} + p^{+}$ --- d^{+} + neutrons (1.44 MeV) and $d^{+} + e^{!}$ --- 2n + ... occurred in Kamada's experiments. In fact, Kamada's experiment provided us with the most favorable conditions under which to examine and consider the new interaction Eq. (9). It gave us, in fact, a deliberate combination of protons and electrons in a physical situation, which promoted wave-function overlap. It clearly illustrated neutron emission from the electrical discharging process to be the result of electron capture within a proton.

CONCLUSIONS

We can confirm from data gathered on neutron production and heat measurement during electric discharge of a Pt electrode in a carbolic acid heavy water solution the following: The emission of low energy neutrons following high voltage discharge was noted after several tens of seconds of discharging. Emission levels fluctuated greatly and neutron energy extended in range from thermal to fast. Generation of excess heat also fluctuated considerably. The reaction is 100% reproducible.

ACKNOWLEDGMENTS

This research was supported by the Thermal and Electric Energy Technology Foundation and The Institute of Applied Energy. The authors acknowledge the collaboration of Dr. Michio Enyo and Dr. Hiroo Numata.

REFERENCES

1. M. Fleishmann and S.J. Pons, *Electroanal. Chem.*, vol 261, p 301, 1989.
2. S.E. Jones et al, *Nature*, vol 228, p 737, 1989.
3. V.A. Klyuev et al., *Sov. Tech Lett*, vol 12, p 551, 1986.
4. T. Mizuno, T. Akimoto and N. Sato, *Denki Kagaku*, vol 57, p 742, 1989.
5. I.S. Jasnogorodski, *Electrolytisches Hatten*, 1951.
6. N.H. Polakowski, *Met. Plogr.*, vol 67, p 98, 1955.
7. S. Owaku and K. Kuroyanagi, *J.J. Met. Soc.*, vol 20, p 63, 1955.
8. T. Maoka and M. Enyo, *J. Electroanal. Chem.*, vol 108, p 277, 1980.
9. M. Enyo, *J. Electroanal. Chem.*, vol 134, p 75,1982.
10. T. Mizuno and M. Enyo, "Sorption of Hydrogen On and In Hydrogen-Absorbing Metals in Electrochemical Environments," Modem Aspects of Electrochemistry, vol 30, p 415. Ed., J. O'M. Bockris and C. White, Plenum Publishing Corporation, 1996.
11. M. Enyo and P.C. Biswas, "Hydrogen Absorption in Pd Electrode in Alkaline Solutions," *J. Electroanal. Chem.,* vol 335, p 309, 1992.
12. M.H. Mintz, *J. Alloys and Compounds*, vol 176, p 77, 1991.
13. J.O'M. Bockris and R. Sundaresan, "Electrochemistry, Tritium and Transmutation," Cold Fusion Source Book (ed. by H. Fox), Int. Symp. on Cold Fusion and Adv. Energy Sources, Minsk, Belarus, May 1994.
14. E. Rutherford, *Proc. Roy. Soc.*, A97, p 374, 1920.
15. E. Conte, *Physics Essays,* vol 5, p 70, 1992.
16. N. Gisin, *J. Phys. A.*, vol 19, p 205, 1986.
17. K. Kamada, H. Kinoshita and H. Takahashi, *Jpn. J. Appl. Phys.*, vol 33, p 143, 1996.

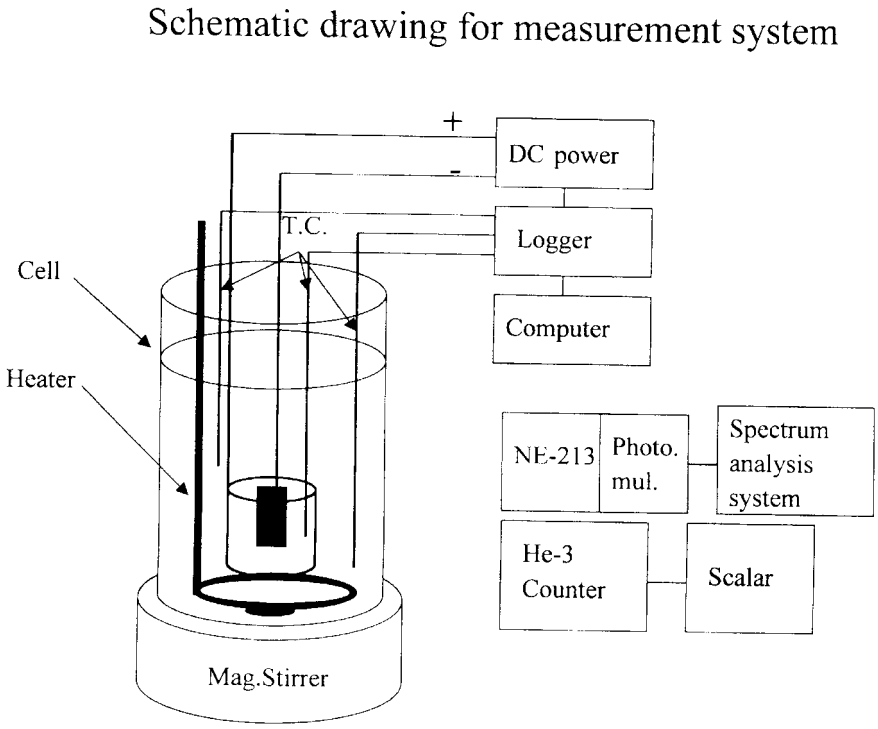

Fig. 1. Schematic drawing of measurements system; the system is surrounded with plastic bricks and set in a constant temperature room

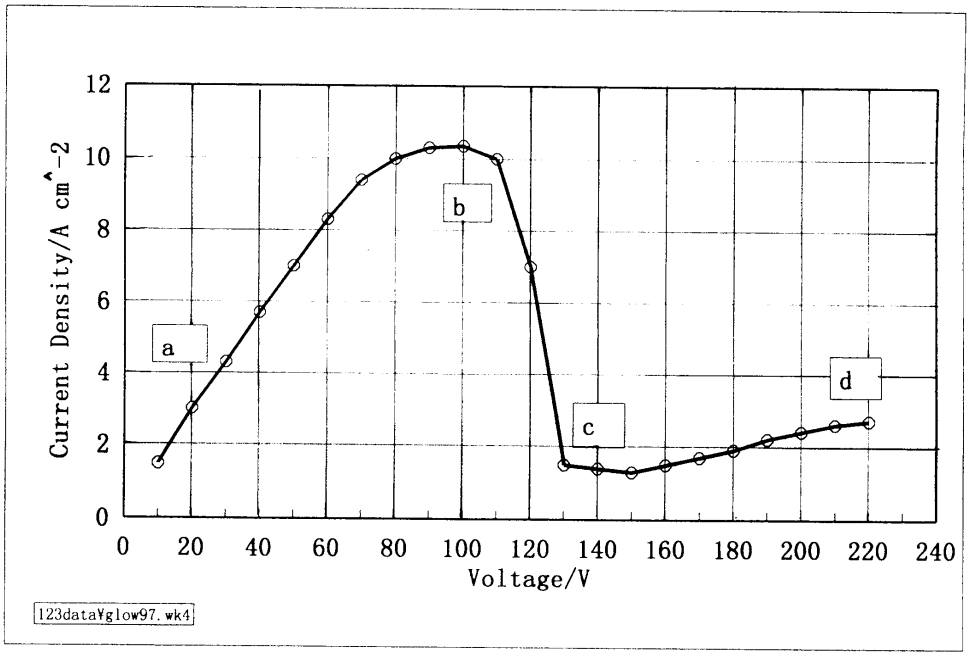

Fig. 2. Current-voltage relation of cathodic discharge in lithium hydroxide solution. Range a-b, normal hydrogen evolution, Range b-c, unstable, Point c radiation start and range c-d is stable radiation.

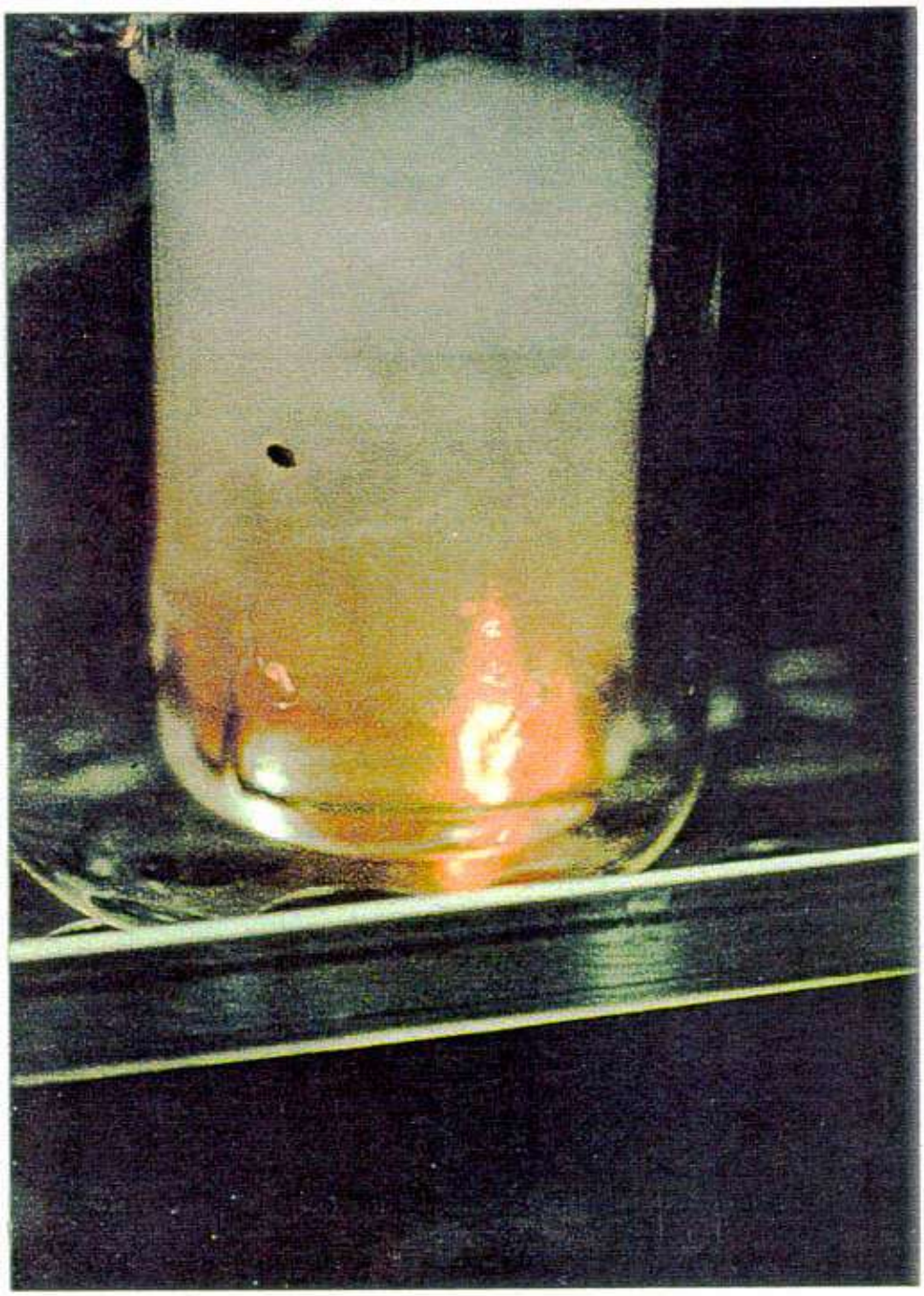

Fig.3. Typical radiation during electrolytic discharging of platinum plate in lithium- hydroxide heavy-water solution.

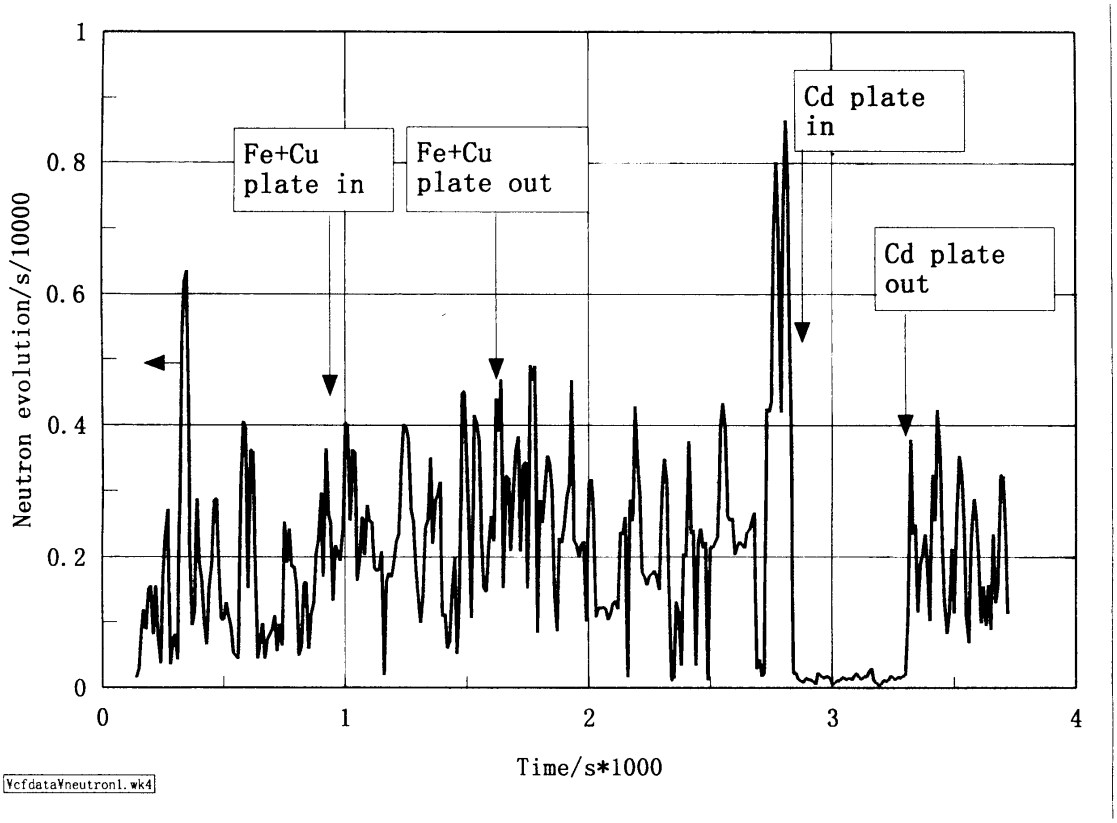

Fig. 4 Time deviation of the neutron evolution; each arrow shows noise and thermal neutron controlling by metal absorbers.

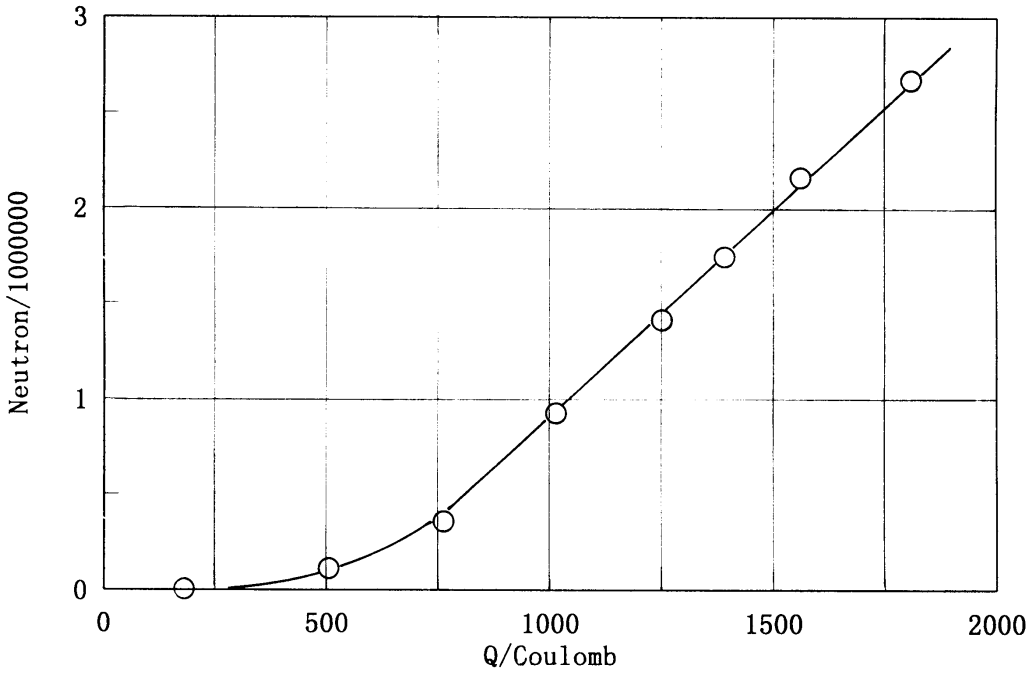

Fig. 5. Gamma-ray emission from the gold plate for the after and the before being irradiated by neutron emission from the cell for 6 hours.

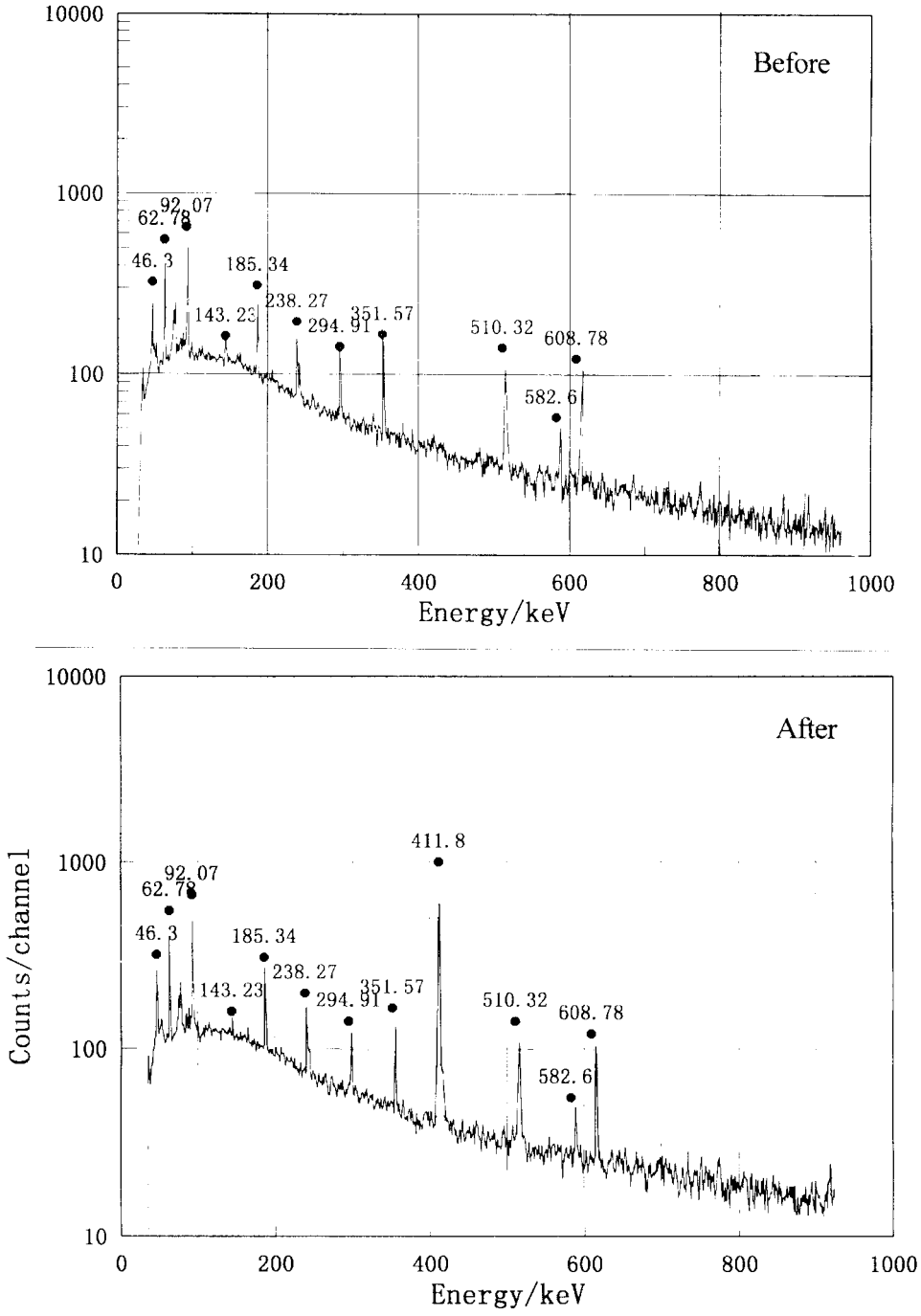

Fig. 6. Neutron evolution and input electric charge relation; neutrons were evolved after some induction periods.

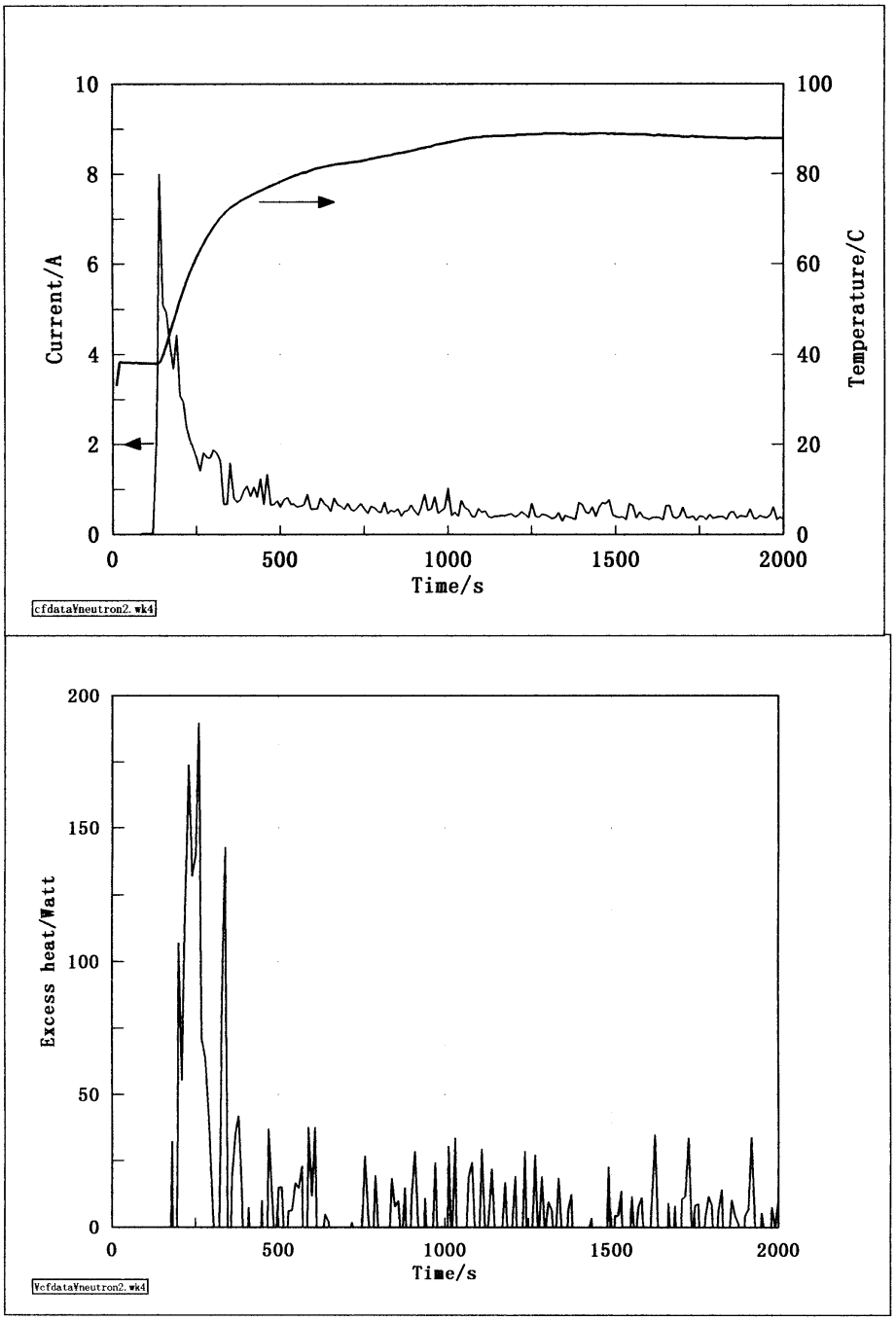

Fig. 7. Time change of the temperature, current (above figure) and the excess heat generation (bottom figure).